Wear resistance of nanostructured Cr-based WC hardmetals sintered by spark plasma sintering

Xiangxing Deng[a,d,*], Núria Cinca[b], Dariusz Garbiec[c], José Manuel Torralba[a,d], Andrea García-Junceda[a]

[a] IMDEA Materials Institute, Calle Eric Kandel 2, 28906 Getafe, Madrid, Spain
[b] Hyperion Materials & Technologies, Polígono Industrial Roca Calle Verneda S/N, Martorelles 08107, Barcelona, Spain
[c] Łukasiewicz Research Network - Metal Forming Institute. Jana Pawla II 14, 61-139, Poznan, Poland
[d] Universidad Carlos III Madrid, Av. Universidad 30, 28911, Leganés, Madrid, Spain.

ARTICLE INFO

ABSTRACT

Nanostructured Cr-based WC hardmetals are successfully sintered by spark plasma sintering. The wear behaviour of these Cr-based WC hardmetals with different C contents ranging from 5.57 wt% to 6.91 wt%, is evaluated performing sliding wear tests under two different wear conditions. This work analyses the influence of the C content on the wear performance through the study of the phase formation and WC grain size. The Cr-based hardmetal with 5.57 wt% C content exhibits a lower wear rate than Co-based WC hardmetals tested under similar dry ball-on-plate wear conditions, even considering that these Co-based WC hardmetals have higher WC content (90 wt%) than Cr-based WC hardmetals (83.2 wt%). The combination of a nanosized WC grain and the avoidance of brittle $(Cr,Fe)_7C_3$ or soft graphite phases leads to a superior wear performance. Thus, the use of Cr-based binders in the hardmetal industry, alternatively to Co-based binders, is promising in applications in which high wear resistance is needed.

1. Introduction

WC-based hardmetals are widely used as cutting tools for metals, plastics and composite due to their high hardness and wear resistance [1]. The wear performance plays a key role for cutting tools in determining the span of life, machining efficient, surface quality, cost and accuracy [2]. Wear characteristics of WC-based hardmetals have been extensively studied under dry conditions using different tribological systems. Jia and Fischer [3] tested the wear resistance of nanostructured and conventional hardmetals on a pin-on-disk tribometer in an unlubricated atmosphere. Liu et al. [4] studied the wear behaviours and mechanisms of WC-Co and WC-Fe$_3$Al hardmetals under a dry sliding system using a ball-on-disc configuration. Bonny *et al* [5,6] conducted wear experiments on WC-Co hardmetals in dry reciprocating sliding contact using a high-frequency TE77 pin-on-plate system. All above references demonstrated that wear performance of hardmetals is directly determined by their chemical composition, phase formation, WC grain size and extra refractory carbide additions, although there were some differences in the tested parameters, counterpart materials and the applied tribological equipment [7]. Generally, the wear

resistance of hardmetals increases with the increase of the WC reinforcement content since the hard WC phase serves as the main counter material [8]. Cobalt binder could reduce the wear resistance and oxidation of hardmetals due to its limited hardness and its poor oxidation resistance, despite it is the most used binder alloy as a consequence of the good wettability of tungsten carbide by cobalt [9,10]. Great interest has been driven to improve the wear resistance of hardmetals without or with less Co contents, especially at high temperatures and under oxidative environments [11,12]. Many researchers have reported that the wear resistance of hardmetals could be significantly improved when the average WC grain becomes nanometric [3–7], [13–15]. More specifically, the benefit of the grain size reduction to nanoscale on the improvement of wear resistance was described as caused by an increase of hardness without reducing the toughness [16]. Two main ways have been performed to reduce the final WC grain size in hardmetals towards nanometric scale: the addition of grain growth inhibitors such as Cr_3C_2 or VC [17], and the application of field-assisted solid state sintering techniques such as spark plasma sintering (SPS) [18,19]. Thus, the addition of chromium or chromium carbides was known as a way to inhibit the growth of WC particles during solid state

Table 1

Designed C contents, real carbon contents measured by LECO, hardness, fracture toughness, and average WC grain size of Cr-based WC hardmetals [24].

Hardmetals	Designed C content (wt%)	Measured C content (wt%)	Hardness (HV30)	Toughness (MPam$^{1/2}$)	Average WC grain size (nm)
Cr-based WC-0.5C	5.59	5.57 ± 0.05	2219 ± 16	8.2 ± 0.1	100 ± 14
Cr-based WC-1C	6.03	6.17 ± 0.09	2164 ± 31	7.4 ± 0.2	350 ± 20
Cr-based WC-2C	6.96	6.91 ± 0.04	1914 ± 13	7.1 ± 0.3	750 ± 85

sintering [20]. Such previous works report to have produced WC-based hard materials with Cr-based alloy by using SPS technique and this Cr-based WC hard composite exhibited a good combination of mechanical properties and oxidation resistance, due to the existence of a nanoscale WC grain size [21,22].

The main goal of the present work is to study the wear behaviour of SPSed Cr-based WC hardmetals with different C contents under dry sliding tests using two different trybosystem conditons. The wear performance of Cr-based WC hardmetals will be compared with Co-based WC hardmetals under similar test conditions, in order to evaluate the prospect of introducing Cr-based WC hardmetals as cutting tools.

2. Experimental

2.1. Spark plasma sintering of Cr-based WC hardmetals

The mechanically milled nanosized Cr-based WC powders with different extra C contents were sintered with full density by SPS at 1350 °C for 10 min, with an applied pressure of 80 MPa. The material designated as Cr-based WC-0.5C in Table 1 has an extra 0.5 wt% C content, whereas others have 1 wt% and 2 wt% extra C contents, respectively. The C content represented was added in Cr-based WC hardmetals. The real C contents in sintered samples were measured by a LECO chemical analyser. The grain size of WC was determined using the linear intercept method on SEM images [23]. Thus, Table 1 lists the designed C contents, the real carbon contents, the hardness values and fracture toughness values by Palmqvist method reported in the previous study [24] together with the average WC grain size of the Cr-based WC hardmetals used in this work.

2.2. Wear resistance tests

The studies of wear resistance shown in this research were carried out using two equipments with different specimen sizes: samples with 6 × 5 × 4 mm for wear tests in a Bruker-UMT-Tribolab trybometer and samples with 20 × 6.5 × 6 mm for wear tests developed in a Wazau-TRM 2000-Tribometer. Both wear measurements on Cr-based WC hardmetals are characterised by dry sliding tests on a ball-on-plate configuration using reciprocating lineal movement. Prior to the tribological test, samples were polished and cleaned in distilled water for 10 min followed by drying in furnace at 110 °C for 30 min. An alumina ball of 5 mm diameter (supplied by Goodfellow) was used as a static counter material in the Bruker tribometer. The samples were moving against the alumina ball reciprocally. The tests were performed in ambient air (20 ± 2 °C, humidity 55%), under 15 N or 18 N load, at a frequency of 5 Hz, and the stroke length was of 5 mm for 30 min. All tests were repeated 3 times in order to have repeatability in terms of the friction coefficient (μ). The total sliding distance was fixed to 90,000 mm. A WC-6 wt% Co ball of 10 mm diameter (supplied by Fritsch) was used as a static counter material in the Wazau tribometer. These tests were performed in ambient air under 50 N load, at a frequency of 2.5 Hz, and a stroke length of 10 mm for 60 min in ambient air (20 ± 2 °C, humidity 55%). The total sliding distance was fixed to 100,000 mm.

A profilometer (Olympus DSX500, Opto-digital microscope) was used to obtain the 3D images of the wear tracks after sliding. The values of width, depth, and volume loss were determined by three 2D profiles, which were obtained from the 3D image. Then, the average depth value was calculated by the following Eq. [25]:

$$\overline{D} = \frac{\overline{A_w}}{\overline{W}}$$

where $\overline{D}$ is the average depth in mm, $\overline{A_w}$ is the average wear loss area of three 2D profiles for each wear track, and $\overline{W}$ is the average width of each wear track measured for three 2D profile. Thus, the wear loss volume is calculated with the following formula:

$$\Delta V = \left[\frac{1}{3} \times \pi \times \overline{D}^2 (3R - \overline{D}) \right] + \overline{A_w} \times l$$

where ΔV is the volume loss for wear sliding in mm^3, R is the radius of the sliding ball, and l is the sliding stroke. The wear rate is determined by the following formula [26]:

$$W_v = \frac{\Delta v}{FS}$$

where W_v is the wear rate in mm^3/mm, ΔV is the volume loss of the sample in mm^3, F is the contact load and S is the total sliding distance. We need to mention that the oxidation of the binder phase during dry sling wear testing may affect the measurement of volume loss due to its high Pilling-Bedworth ratio [27].

3. Results and discussion

3.1. Microstructural analysis of the SPSed Cr-based hardmetals

Fig. 1 displays the microstructure of Cr-based WC hardmetals with
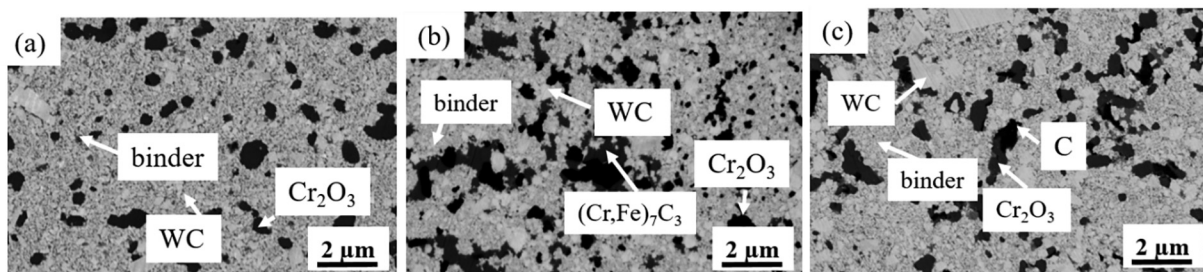

Fig. 1. BSE images revealing the microstructure of Cr-based WC with different C contents: (a) 5.57 wt%, (b) 6.17 wt%, and (a) 6.91 wt%; white phase is WC, grey is (Cr,Fe)$_7$C$_3$, and dark is Cr$_2$O$_3$ or graphite.
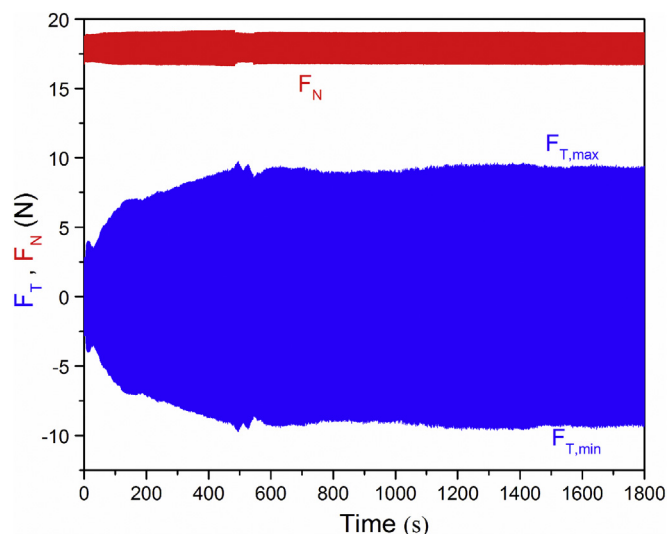
Fig. 2. Real time normal force (F_N) and friction force (F_T) for a load of 18 N, frequency of 5 Hz, stroke length of 5 mm, as a function of time for Cr-based WC hardmetals [6].
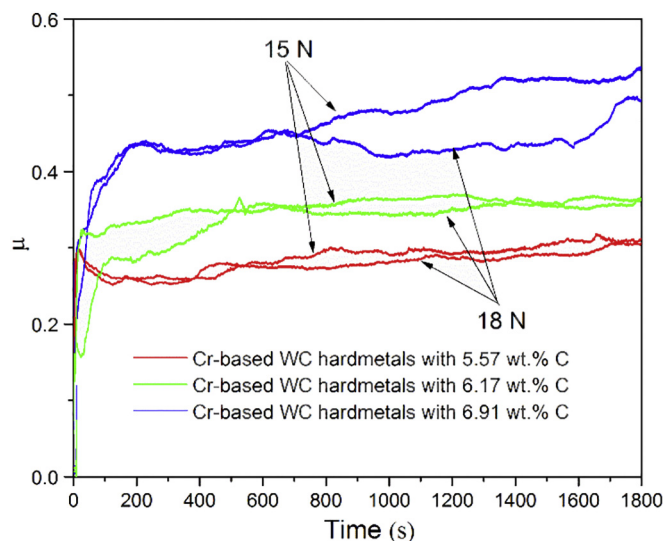

Fig. 3. Friction coefficient as a function of time for two different contact loads (15 N and 18 N) in Cr-based WC hardmetals with different C contents tested using an alumina ball, a frequency of 5 Hz, and stroke length of 5 mm for 30 min.

different C contents. The Cr-based WC hardmetal with 5.57 wt% C content consists of WC, binder and Cr_2O_3 phases, with an average WC grain size of 100 nm. A $(Cr,Fe)_7C_3$ phase (grey region) and graphite (dark) are formed in Cr-based WC hardmetal with 6.17 wt% and 6.91 wt% C, respectively. The formation of brittle $(Cr,Fe)_7C_3$ or soft graphite is detrimental for the mechanical properties of hardmetals. The average WC grain size also increases with the increase of C content from 100 nm to 750 nm, which may due to a better solubility of WC grains and more effective growth of WC in the Cr-based alloy [20].

3.2. Dry ball-on-plate wear test under the mild aggressive conditions

3.2.1. Friction coefficient and wear surface analyses

The imposed normal force (F_N) and the concomitant tangential friction force (F_T) of the count ball part were continuously recorded using a load and a friction sensor [6], respectively, when a load of 15 or 18 N was applied against Cr-based WC hardmetals. The static friction force (F_T) is calculated using the following equation:

$$F_T = \frac{|F_{T,max}| + |F_{T,min}|}{2}$$

The coefficient of friction (μ) is calculated from the F_T/F_N ratio. Fig. 2 shows that the recorded normal contact force seems to correspond very well to the imposed contact load of this particular case, which is 18 N. The friction force appears either positive or negative, depending on the sliding direction.

The evolution of the friction coefficient (μ) for Cr-based WC hardmetals with different extra carbon contents is displayed in Fig. 3. Two loads (15 N and 18 N) are applied to study the effect of force on the friction coefficient, μ. Generally, the friction coefficient increases rapidly throughout the first seconds, which is attributed to the quick increase of theball-on-disc contact area due to polishing of asperities [6]. After the initial stage, the variations in μ become smaller in the "running in" stage, and it reaches an equilibrium state of stable value, since the wear track becomes smoother after ploughing away the surface asperities [5]. However, the friction coefficient observed in Cr-based WC hardmetals with 6.91 wt% C content appears slightly inconstant due to the existence of soft graphite phase. Thus, the surface with graphite has less resistance to overcome, which leads to an increase in surface roughness, and therefore the μ increases [5]. Fig. 3 highlights that a higher contact load (18 N) leads to smaller and more stable values of friction coefficient, since the increase in F_T is lower than that in

F_N when the applied force increases. Thus, the higher load of 18 N is selected as the force to be applied on all Cr-based WC hardmetals in the next analyses. The friction coefficients measured for Cr-based WC hardmetals with 5.57 wt% C, 6.17 wt% C, and 6.91 wt% C contents are in the range of 0.27–0.30, 0.34–0.36, and 0.43–0.51, respectively, due to the different phases existing in each material which may have a distinctive effect on the friction coefficient [13]. $(Cr,Fe)_7C_3$ and graphite exist in the Cr-based WC hardmetals with extra 6.17 wt% C and 6.91 wt% C, respectively, which increases the F_T due to their lower levels of hardness compared to that of WC, finally leading to the increase of the friction coefficient.

Visual observations after the wear sliding tests reveal a smooth and bright appearance of the wear track in all tested samples, indicating that the surfaces of Cr-based WC hardmetals have been ploughed by the alumina ball during the wear sliding. SEM and EDX analyses are performed on the worn surfaces to obtain more information of the wear process followed. Fig. 4 illustrates general images of the worn surfaces and a higher magnification of the central part in the wear track. From the general view of the wear tracks, a slight decrease of the wear track width with the increase of the carbon content (the distance between two white dashed lines in Fig. 4) is found for Cr-based WC hardmetals. The width varies from a value around 200 μm, in samples with extra 0.5 wt% C content, to around 170 μm and 165 μm, in samples with 6.17 and 6.91 wt% C contents, respectively. This phenomenon can be explained by the occurrence of different mechanisms: abrasive wear, adhesion of wear debris layers, soft phase removal, and grain cracking. The parallel grooves in all the wear tracks point out that the abrasive wear mechanism is dominant in all Cr-based WC hardmetals. The Cr-based WC hardmetal with 5.57 wt% C content has the highest hardness, as previously reported, which leads to an increase in the wear track width due a higher volume loss coming from the alumina ball. The BSE and SE micrographs in the central part of the worn surface in the Cr-based WC hardmetals with extra 5.57 and 6.17 wt% C contents show the adhesion of the wear debris layers in grey color. Actually, the existence of thin wear debris layers on the surface of hardmetals protects the Cr-based WC hardmetals, leading to an improvement of their wear resistance [6]. On the other hand, the presence of $(Cr,Fe)_7C_3$ phase and the bigger WC grain size will decrease the wear resistance of Cr-based WC hardmetals when extra C increases from 0.5 to 1 wt%, due to the less hardness and fracture toughness [24]. BSE and SE micrographs of worn surface in Cr-based WC hardmetals with 6.91 wt% C content,
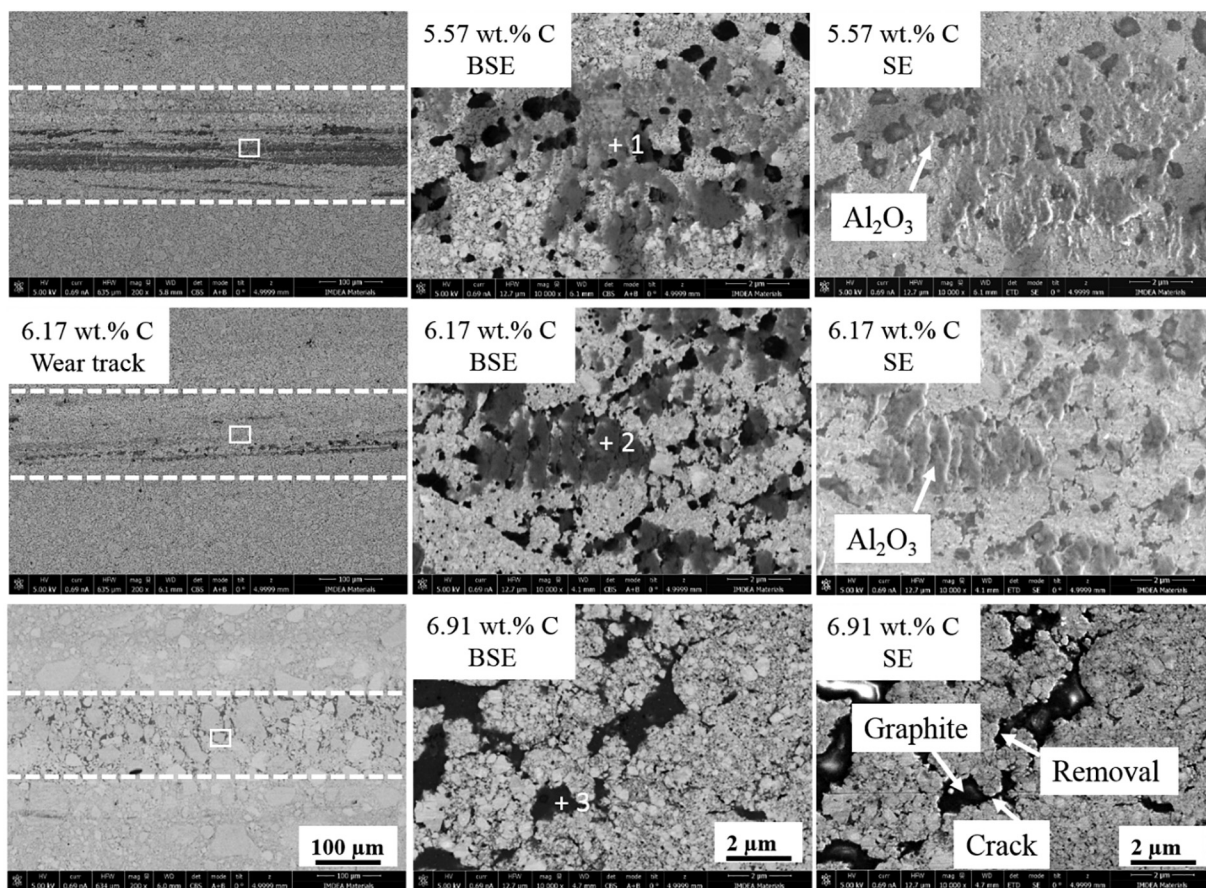
Fig. 4. BSE and SE images of the wear track generated in Cr-based WC hardmetals with different C content after wear tests with a load of 18 N, frequency of 5 Hz, stroke length of 5 mm, and time of 30 min. General view images of wear track on the left and higher magnification of the central part in wear track (white square area) on the right. EDX point analyses are carried out in the positions of numbered as 1, 2, and 3.
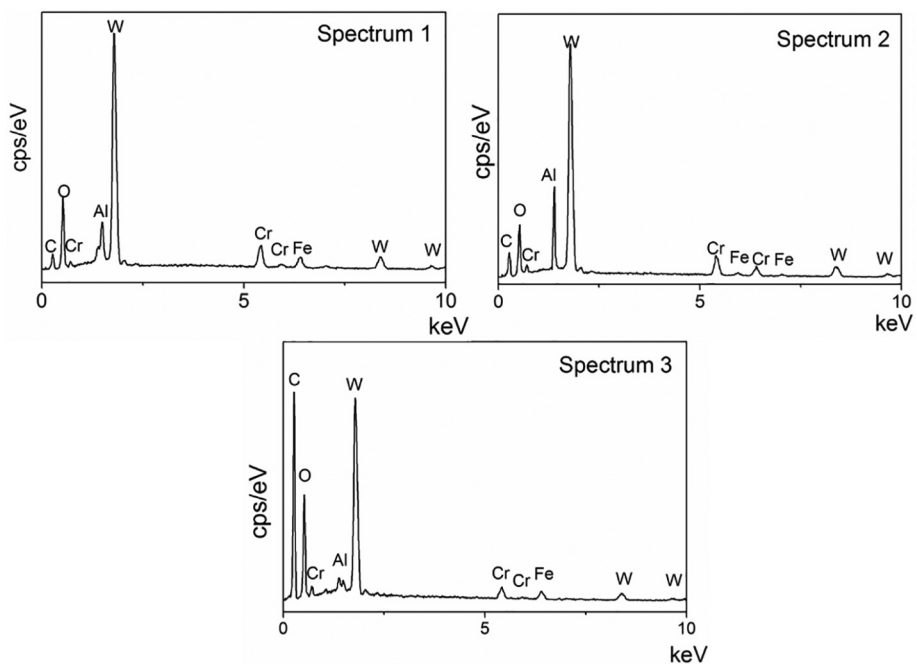

Fig. 5. EDX analyses on wear tracks corresponding to Cr-based WC hardmetals with 5.57 wt%, 6.17 wt% and 6.91 wt% C contents, respectively.
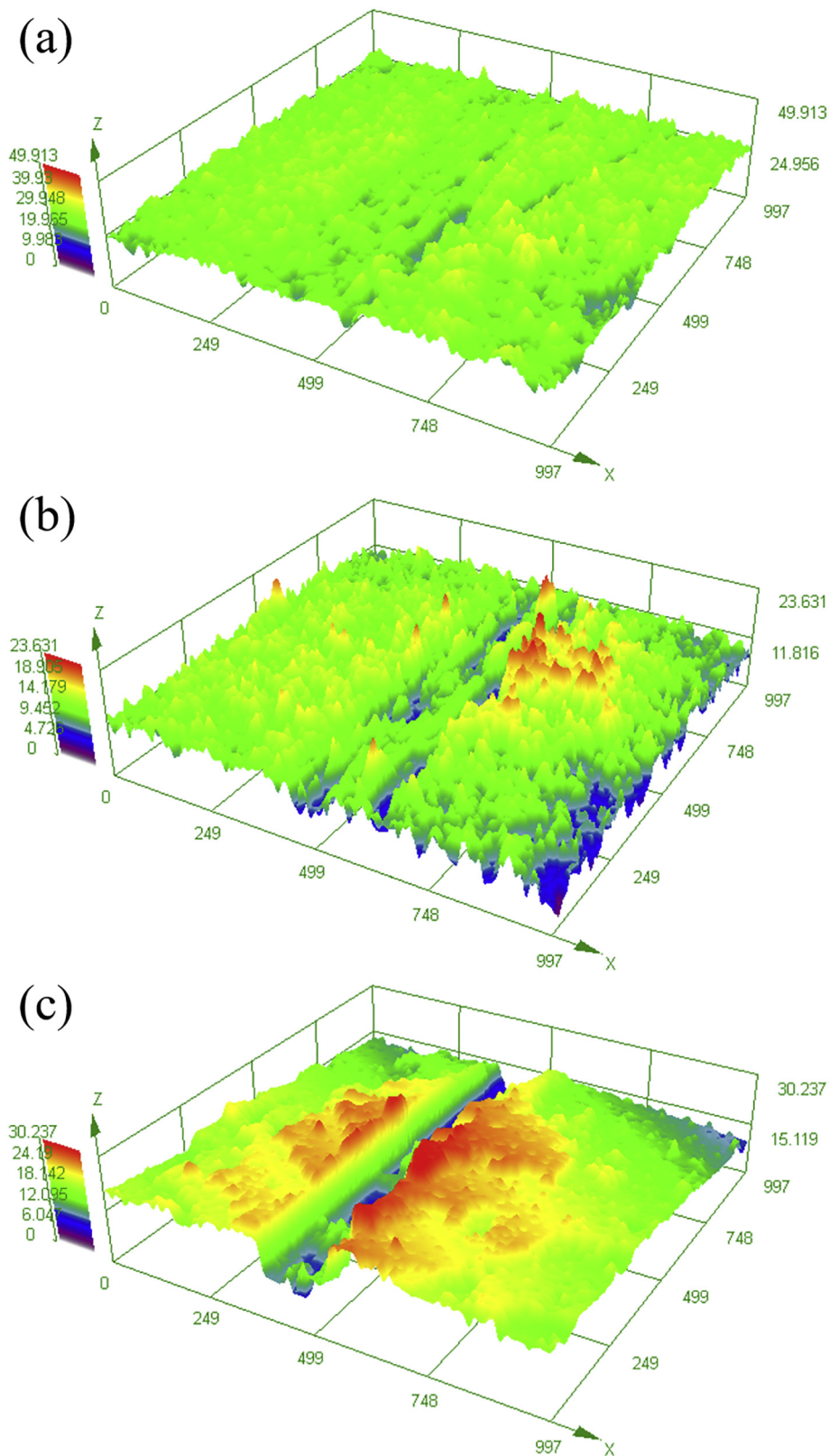
Fig. 6. 3D topographic images showing the wear tracks of Cr-based WC hardmetals with different extra C contents after dry sliding tests with a load of 18 N, frequency of 5 Hz, stroke length of 5 mm, and time of 30 min: (a) 5.57 wt% C, (b) 6.17 wt% C, and (c) 6.91 wt% C.

present micro cracks and surface removal of the soft graphite, which lead to a further grain pullout and reduction of wear resistance. Additionally, the removal of the binder and/or graphite phase increases the tangential friction force, leading to a higher friction coefficient, which explains the trend followed by the friction coefficient displayed in Fig. 3.

EDX spectrum 1, taken in the worn surface of the Cr-based WC hardmetal with 5.57 wt% content, reveals the existence of W, Al, Cr, O,
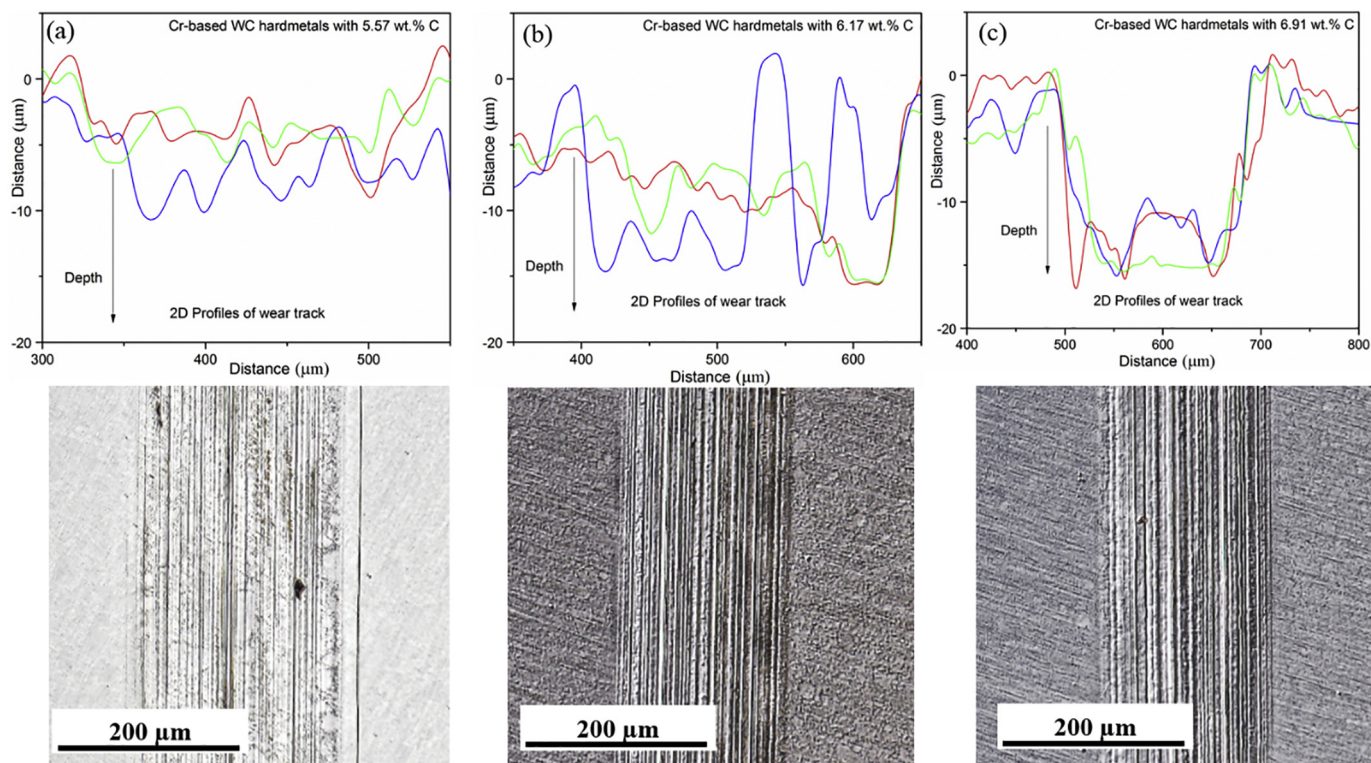
Fig. 7. Representative wear track profiles and corresponding optical images of Cr-based WC hardmetals with different extra C contents after dry sliding tests with a load of 18 N, frequency of 5 Hz, stroke length of 5 mm, and time of 30 min: (a) 5.57 wt% C, (b) 6.17 wt% C, and (c) 6.91 wt% C.

Table 2
Wear data obtained for Cr-based WC hardmetals with extra 0.5, 1, and 2 wt% C contents tested with a load of 18 N, frequency of 5 Hz, and stroke length of 5 mm against alumina ball.

Cr-based WC hardmetals with different C contents	Width $\overline{W}$ (µm)	Loss area $\overline{A_w}$ (µm²)	Depth $\overline{D}$ (µm)	Volume loss $\overline{\Delta V}$ (10^{-6} mm³)	Wear rate $\overline{W_v}$ (10^{-9} mm³/N·m)
(0.5 wt% C)	217.4 ± 3	1047.6 ± 226	4.7 ± 0.2	5.2 ± 0.2	3.2 ± 0.1
5.57 wt% C	212.2 ± 5	1107.7 ± 326	5.2 ± 0.4	5.6 ± 0.4	3.4 ± 0.2
	192.7 + 7	1007.7 ± 287	5.1 ± 0.2	5.1 ± 0.2	3.2 ± 0.1
(1 wt% C)	173.6 ± 4	1407.6 ± 187	8.1 ± 0.2	7.0 ± 0.4	4.3 ± 0.3
6.17 wt% C	178.0 ± 5	1307.7 ± 214	7.3 ± 0.2	6.5 ± 0.3	4.1 ± 0.2
	180.6 ± 3	1387.1 ± 314	7.6 ± 0.2	6.9 ± 0.1	4.2 ± 0.2
(2 wt% C)	169.0 ± 4	2047.6 ± 385	12.0 ± 0.4	9.5 ± 1.0	6.0 ± 0.2
6.91 wt% C	153.9 ± 5	2243.7 ± 585	14.5 ± 0.2	9.6 ± 1.2	5.9 ± 0.2
	170.0 ± 3	2368.5 ± 701	13.9 ± 0.8	10.5 ± 0.5	6.5 ± 0.3

Fe and C, as shown in Fig. 5. Therefore, the wear surface is enriched in Al and O content, coming from the alumina ball. Hence, the worn track surface turns to be covered with a thin Al_2O_3 wear debris layer, separating the Cr-based WC hardmetal from the count sliding ball. It is worth noting that a similar EDX spectrum is obtained in the wear track of the Cr-based WC hardmetal with 6.17 wt% C content (spectrum 2). The spectrum 3, taken in the crack region of the hardmetal with 6.91 wt % content, reveals more quantity of C and O, and less Al since graphite is being removed from the bulk material and probably it is covering the wear track. In fact, the micro-cracks presented in this hardmetal are induced by tangential stresses due to the reciprocal sliding contact pressure exerted by the alumina ball, which leads to the removal of the soft graphite.

3.2.2. Volume loss and wear rate

Fig. 6 shows the 3D topographic images of the worn surfaces for Cr-based WC hardmetals with different C contents after dry sliding tests. The different colors in the topographic images are related to the distribution of heights: red represents the highest height, while purple indicates the lowest height. As expected, severe parallel grooves are observed in the wear tracks since abrasion wear is the main mechanism for the surface sliding against alumina ball. Fig. 6(c) highlights that the worn surface of the Cr-based WC hardmetal with 6.91 wt% C content exhibits the narrowest and deepest wear track, whereas the Cr-based WC hardmetal with 5.57 wt% C content has the widest and shallowest one, as shown in Fig. 6(a). Therefore, the results shown in Fig. 6 suggest that the volume loss of Cr-based hardmetals increases with the increase of the C content from 5.57 to 6.91 wt%.

Fig. 7 presents the wear track profiles taken in three different intersection lines and the corresponding optical images of the wear tracks in Cr-based WC hardmetals with different C contents after dry sliding tests. The average width of the track and the average wear loss area of each profile are measured by surface profilometry, and results are listed in Table 2. This table summarises the average width, loss area, depth, wear volume loss, and wear rate values calculated for all the Cr-based WC hardmetals tested during 30 min against an alumina ball with a load of 18 N, frequency of 5 Hz, and stroke length of 5 mm. The lowest depth and volume loss are achieved by the Cr-based WC hardmetal with 5.57 wt% C content, whereas the highest values occur for the Cr-based WC hardmetal with 6.91 wt% C content, which is in full agreement with
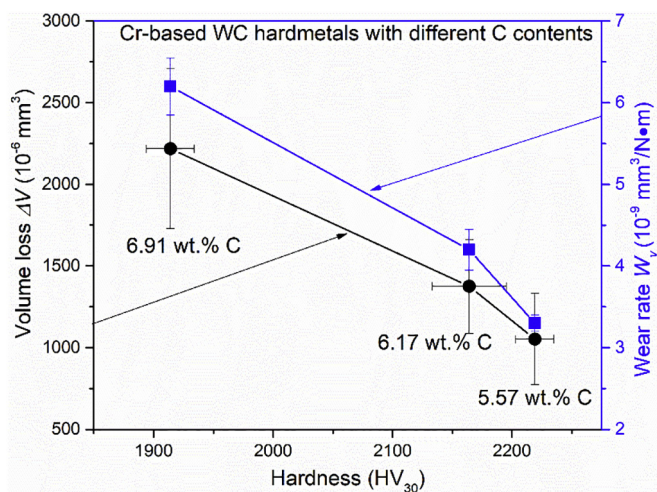
Fig. 8. Volume loss and wear rate against hardness after dry sliding tests with a load of 18 N, frequency of 5 Hz, stroke length of 5 mm, and time of 30 min in Cr-based WC hardmetals with 5.57, 6.17 and 6.91 wt% C contents.
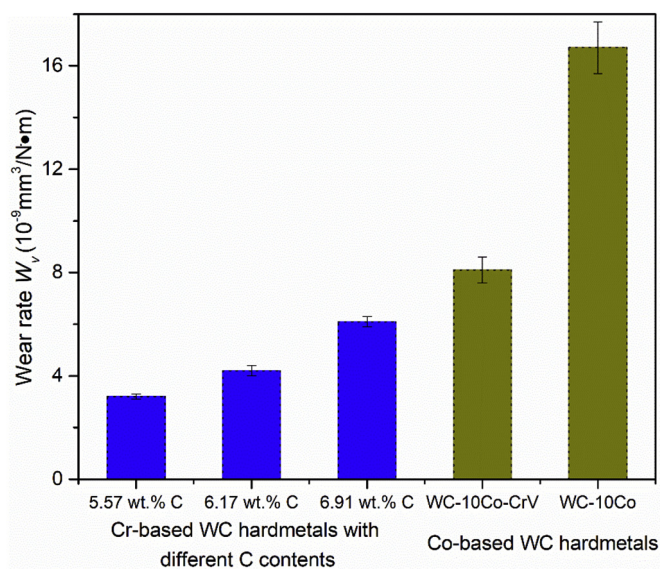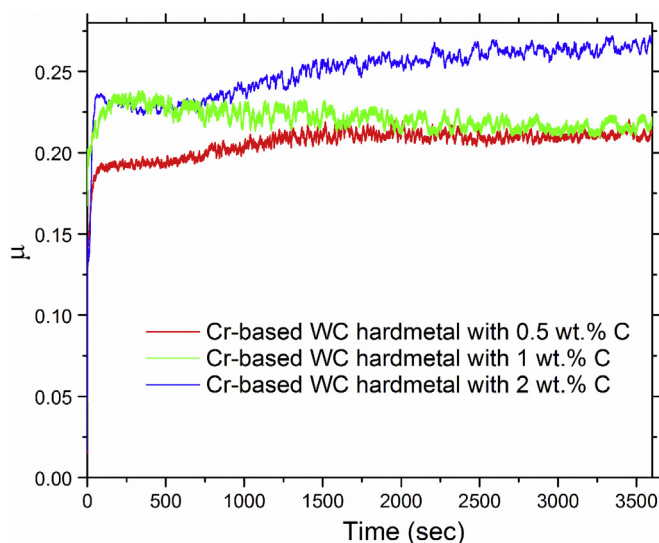

Fig. 10. Friction coefficient (μ) against time in Cr-based WC hardmetals with different extra C contents tested using a WC-Co ball with a load of 50 N, frequency of 2.5 Hz, and stroke length of 10 mm for 60 min.

Fig. 9. Wear rate comparison between Cr-based WC hardmetals and Co-based WC hardmetals [5].

the microstructural surface analyses and 3D topographic images previously shown. The volumetric wear rates of Cr-based WC hardmetals with 5.57, 6.17, and 6.91 wt% C contents vary between 3.2 and 3.4×10^{-9}, 4.1–4.3×10^{-9}, and 5.9–6.5×10^{-9} mm^3/N·m, respectively. Therefore, these results remark that the Cr-based WC hardmetal with 5.57 wt% carbon content has the highest wear resistance, which is well consistent with the existence of a uniform nanosized WC grain distribution, with the smallest WC size (around 100 nm), and with the avoidance of graphite.

Many investigations have reported that the wear resistance performance of hardmetals depends on hardness [6,9,28]. Fig. 8 shows the relationship among volume loss, wear rate, and hardness for Cr-based WC hardmetals. Both volume loss and wear rate clearly decrease with the increase of the hardness. Thus, in this work the Cr-based WC hardmetal with the highest hardness (5.57 wt% C content) leads to the highest wear resistance.

Fig. 9 shows the wear rate comparison between Cr-based WC hardmetals and some commercial Co-based WC hardmetals. The corresponding wear rates of Co-based WC hardmetals are transformed into the same unit (10^{-9} mm^3/N·m) [5]. Cr-based WC hardmetals exhibit

better wear resistance performance than Co-based WC hardmetals, even considering that these Co-based WC hardmetals have a higher content of WC (90 wt%) than the Cr-based WC hardmetals (83.2 wt%). As mentioned before, the wear resistance depends on the content, grain size and distribution of WC, increasing dramatically as WC grain size is reduced. Cr-based WC hardmetals have a uniform distribution of nanosized WC grains, leading to a superior wear resistance performance. Among these Cr-based WC hardmetals, Fig. 9 shows that the Cr-based WC hardmetal with and extra carbon content of 0.5 wt% exhibits the lowest wear rate a higher, due to the smallest WC grain size together with the avoidance of $(Cr,Fe)_7C_3$ or graphite.

The previous findings point out that the wear performance of Cr-based WC hardmetals is primary controlled by abrasive wear. Both wear volume loss and wear rate increase with the decrease of hardness. The existence of Al_2O_3 in the surface of the wear tracks confirms that the adhesion of wear debris layers takes place on the Cr-based WC hardmetals, which is beneficial to improve the wear resistance. Microcracks and some surface soft phase removals are detected in the Cr-based WC hardmetal with a 6.91 wt% C. The uniform distribution of nanosized WC grain size in Cr-based WC hardmetals is the key-reason for achieving an excellent wear behaviour, even compared to WC-Co hardmetals with a higher content of WC hard phase.

3.3. Dry ball-on-plate wear test under more aggressive conditions

3.3.1. Friction coefficient and wear surface analyses

Dry ball-on-plate tests are also performed under more aggressive experimental conditions. A WC-6wt%Co ball (diameter of 10 mm) is rubbed in oscillating movement against Cr-based WC hardmetals. In order to study the friction condition of imposed normal contact force on Cr-based WC hardmetals, the evolution of the friction coefficient (μ) against time in Cr-based WC hardmetals is evaluated in Fig. 10. A similar trend in the friction coefficient is observed during the sliding process in all the samples evaluated. The friction coefficient increases quickly in the initial stage due to the increase of the ball-on-disc contact area, and then becomes stable, since the friction force reaches a constant value in the smooth wear track after polishing away the original surface roughness [6]. The friction coefficient in this wear test is lower than in previous one, since the difference in hardness between WC-Co material and the tested samples is smaller than that between Al_2O_3 material and those tested samples. The friction coefficient of Cr-based WC hardmetals increases again slightly with the increase of the C
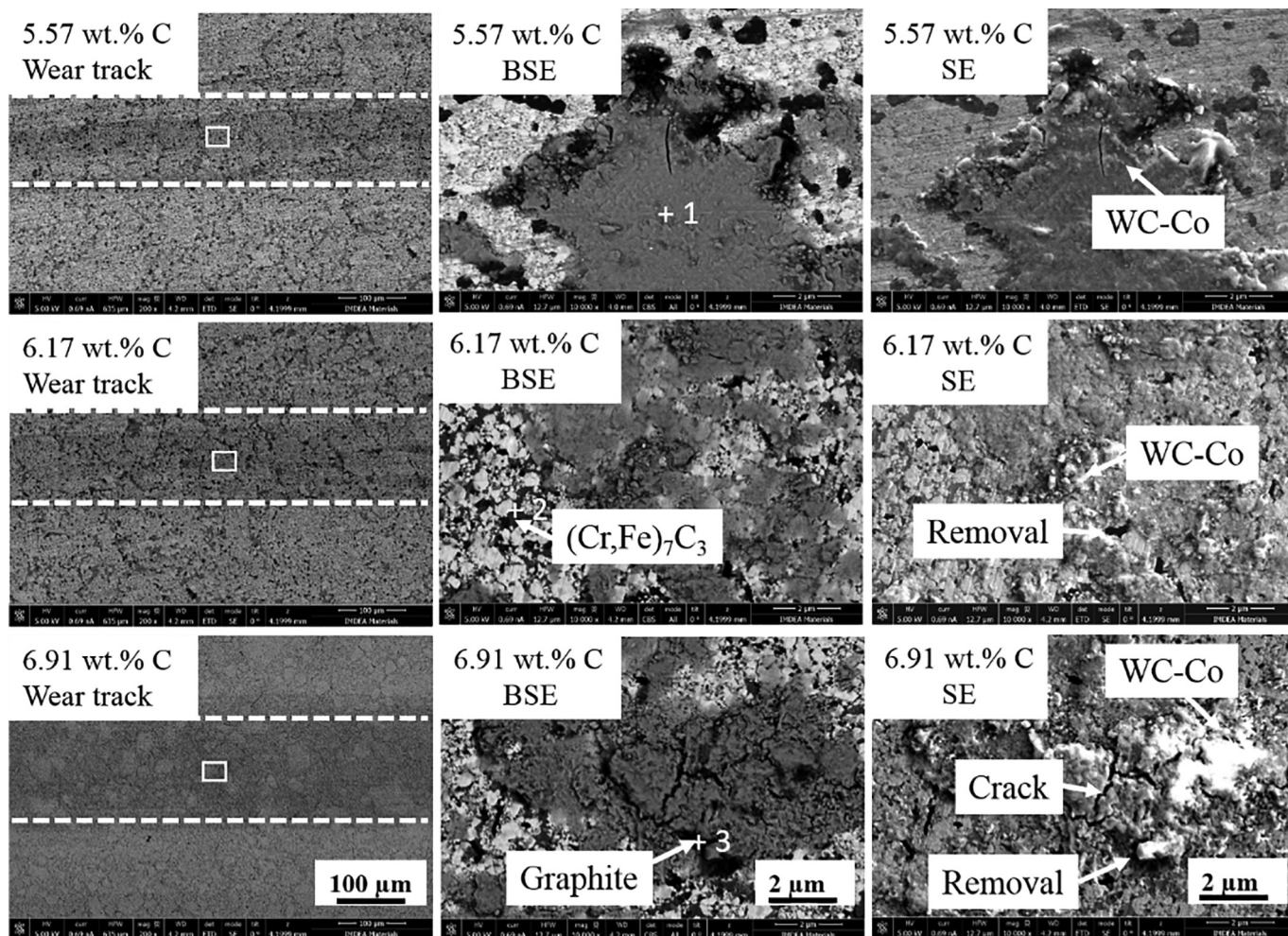
Fig. 11. BSE and SE images of the wear track generated in Cr-based WC hardmetals with different C contents after wear tests with a load of 50 N, frequency of 2.5 Hz, stroke length of 10 mm, and time of 60 min. General view images of wear track on the left and higher magnification of the central part in the wear track (white square area) on the right.
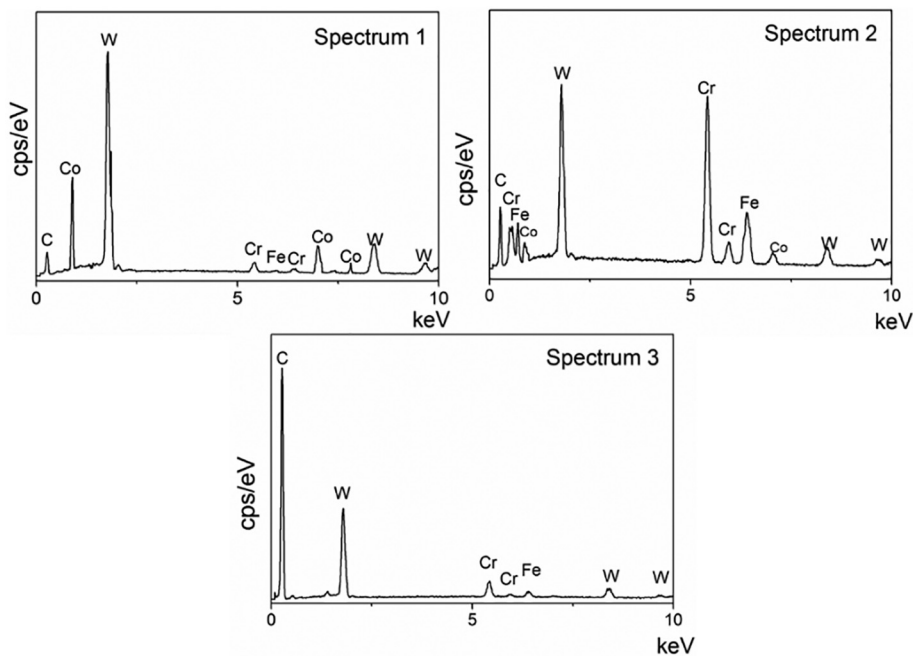

Fig. 12. EDX analyses on wear tracks corresponding to Cr-based WC hardmetals with extra 0.5, 1, and 2 wt% C contents, respectively.
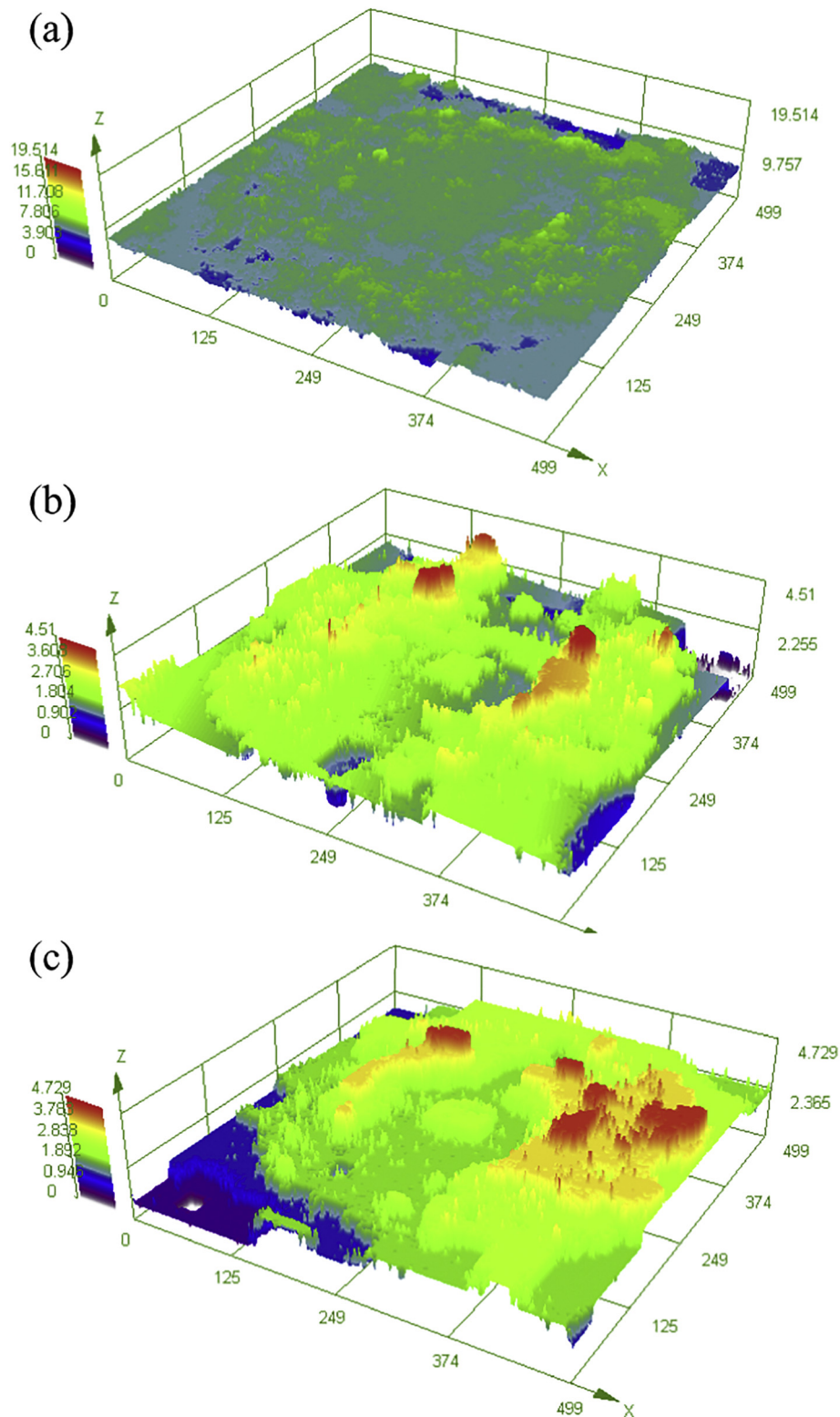
Fig. 13. 3D topographic images showing the wear tracks of Cr-based WC hardmetals with different extra C contents after dry sliding tests with a load of 50 N, frequency of 2.5 Hz, stroke length of 10 mm, time of 60 min: (a) 5.57 wt% C, (b) 6.17 wt% C, and (c) 6.91 wt% C.

content, as a consequence of the existence of larger WC grains and the presence of $(Cr,Fe)_7C_3$ or graphite, which is in good agreement with the previous results obtained under less aggressive conditions.

A smooth and bright wear track is found by visual observation in the surface of each Cr-based WC hardmetal after wear sliding tests. In order to further study the wear surface of Cr-based WC hardmetals, Fig. 11

shows general images of the worn surface and images with a higher magnification of the central part in the wear track. From the general view of the wear track, it can be concluded that the width values (the distance between two white dashed lines) are around 225 μm in all Cr-based hardmetals due to the similar hardness of counter material and tested samples. The abrasive wear mechanism is also dominant in all
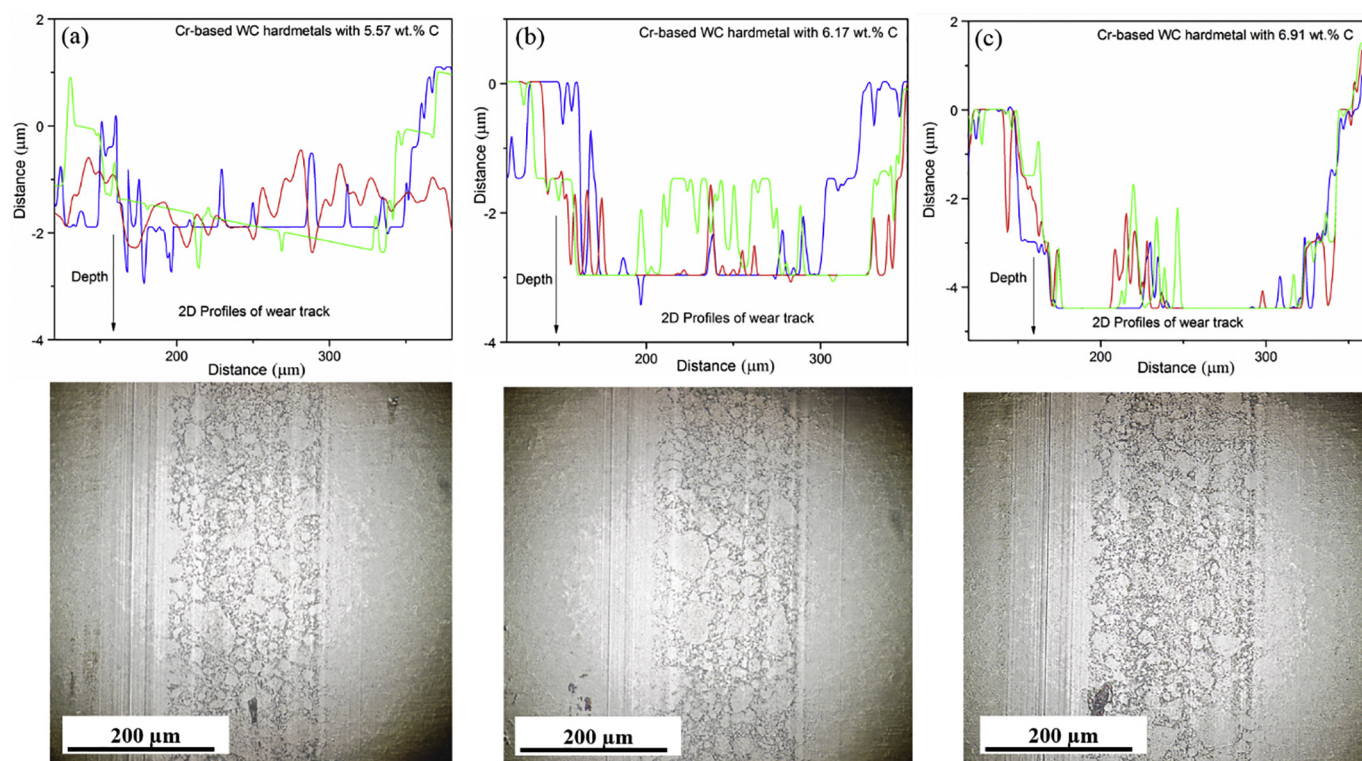
Fig. 14. Representative wear track profiles and corresponding optical images of Cr-based WC hardmetals with different extra C contents after dry sliding tests with a load of 50 N, frequency of 2.5 Hz, stroke length of 10 mm, and time of 60 min: (a) 5.57 wt% C, (b) 6.17 wt% C, and (c) 6.91 wt% C.

Table 3
Wear data obtained for Cr-based WC hardmetals with extra 0.5, 1, and 2 wt% C contents tested with a load of 50 N, frequency of 2.5 Hz, and stroke length of 10 mm against a WC-6Co ball.

Cr-based WC hardmetals with different C contents	Width $\overline{W}$ (μm)	Loss area $\overline{A_w}$ (μm^2)	Depth $\overline{D}$ (μm)	Volume loss $\overline{\Delta V}$ (10^{-6} mm^3)	Wear rate $\overline{W_v}$ (10^{-9} mm^3/N·m)
(0.5 wt% C)	224.4 ± 4	702.1 ± 26	2.3 ± 0.1	7.1 ± 0.2	1.4 ± 0.1
5.57 wt% C	212.2 ± 5	687.2 ± 32	2.4 ± 0.3	6.9 ± 0.4	1.3 ± 0.2
	192.7 + 7	697.0 ± 27	2.5 ± 0.2	7.0 ± 0.2	1.4 ± 0.1
(1 wt% C)	224.1 ± 4	1245.7 ± 57	3.1 ± 0.2	12.5 ± 0.4	2.5 ± 0.3
6.17 wt% C	234.5 ± 5	1307.7 ± 42	3.2 ± 0.2	13.1 ± 0.3	2.6 ± 0.2
	220.7 ± 3	1287.4 ± 34	3.3 ± 0.2	12.9 ± 0.4	2.6 ± 0.2
(2 wt% C)	222.5. ± 4	1929.2 ± 85	4.3 ± 0.4	19.3 ± 0.5	3.9 ± 0.3
6.91 wt% C	233.9 ± 5	2049.3 ± 55	4.5 ± 0.2	20.5 ± 0.8	4.1 ± 0.4
	225.0 ± 3	2074.3 ± 71	4.4 ± 0.3	20.7 ± 0.7	4.1 ± 0.3

Cr-based WC hardmetals, as indicated by the parallel grooves observed in the wear tracks. Adhesion of debris wear layers takes place in all samples, as suggested by the existence of thin WC-Co layers. The Cr-based WC hardmetal with 6.17 wt% C content has suffered the removal of material, whereas it was not detected during the tests with alumina ball at lower load and time. This phenomenon can be attributed to more severe wear conditions, which may cause the removal of the (Cr,Fe)$_7$C$_3$ phase. Growth of cracks and surface phase removal are detected in the Cr-based WC hardmetal with 6.91 wt% C content due to the existence of soft graphite phase.

EDX spectra corresponding to areas in Fig. 11 are obtained in the surface of Cr-based WC hardmetals to identify the composition of the debris layers and the composition near the cracks. Fig. 12 shows that EDX spectrum 1, taken on the worn surface of the Cr-based WC hardmetal with a 5.57 wt% C content, is enriched in Co and W, which demonstrates the existence of a WC-Co debris layer. This WC-Co layer is beneficial to improve the wear resistance, which agrees well the results in the simulation of abrasion to WC-Co hardmetals reported by Pignie et al [29]. The EDX spectra 2 and 3 are taken near the cracks and they confirm the existence of (Cr,Fe)$_7$C$_3$ and graphite in the Cr-based WC

hardmetals with 6.17 and 6.91 wt% C contents, respectively, which may explain the phase removal and the crack growth.

3.3.2. Volume loss and wear rate

Fig. 13 presents the 3D topographic images of the worn surface for Cr-based WC hardmetals tested against a WC-Co ball after dry sliding wear tests using a load of 50 N, a frequency of 2.5 Hz, a stroke length of 10 mm, and a time of 60 min. It clearly shows that the depth of the wear track increases with the increase of the C content, whereas the width keeps a similar value. Hence, the volume loss of Cr-based WC hardmetals increases with the increase of the C content. In order to calculate the values of volume loss and wear rate, three intersection lines are taken across the wear tracks.

Fig. 14 shows the wear track profiles and the corresponding optical images obtained in Cr-based WC hardmetals with different C contents after dry sliding tests. Table 3 summarises all the wear data measured. The wear rates of Cr-based WC hardmetals with 5.57, 6.17 and 6.91 wt % C contents vary between 1.3 and 1.4 × 10^{-9}, 2.5–2.6 × 10^{-9}, and 3.9–4.1 × 10^{-9} mm^3/N·m, respectively.

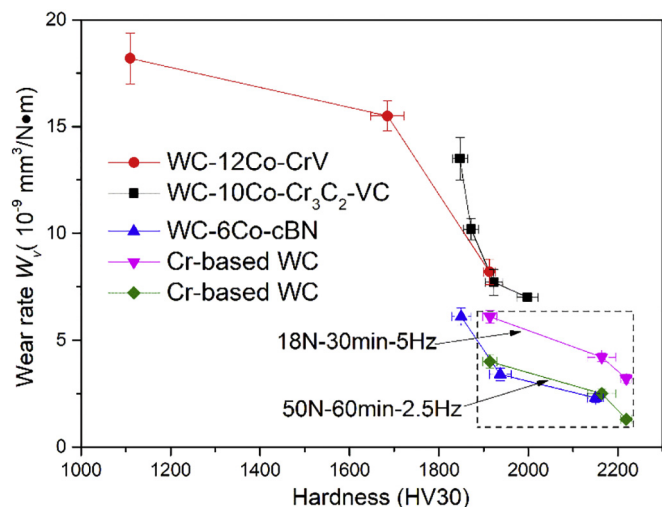Finally, Fig. 15 shows the wear rates of Cr-based WC hardmetals

Fig. 15. Wear rate as a function of hardness for Cr-based WC hardmetals (under different wear conditions marked by the square area) and other Co-based WC hardmetals [5,30,31].

obtained from both wear tests, and the wear rates of some Co-based WC hardmetals found in the literature [5,30,31] under the similar dry sliding conditions. All these Co-based WC hardmetals were obtained by SPS technique with extra addition of refractory carbides (Cr_3C_2, VC, or cBN). As expected, the wear rate generally decreases with the increase of hardness for all hardmetals. The volume loss of Cr-based WC hardmetals increases with the increase of the C content due to the reduction of the hardness. Anyway, the Cr-based hardmetal with 5.57 wt% carbon content under both loading conditions exhibits a lower wear rate than Co-based WC hardmetals tested under similar dry ball-on-plate wear conditions. Thus, the use of Cr-based binders in the hardmetal industry, alternatively to Co-based binders, is promising in applications in which high wear resistance is needed.

4. Conclusions

The wear tests demonstrate that the wear mechanism in Cr-based WC hardmetals is primarily determined by abrasive wear. Adhesion of debris wear layers, soft phase removals, and cracks are confirmed due to the existence of a thin counter material layer, the detection of removed soft phases, and identification of cracks in the microstructure. The adhesion of debris wear layers is beneficial for improving the wear resistance due to the protection of the samples from the sliding materials. The wear rate of Cr-based WC hardmetals increases with the increase of the C content due to the reduction of the hardness as a consequence of the growth of the WC grains from 100 nm to 750 nm and to the existence of phases softer than WC, such as $(Cr,Fe)_7C_3$ or graphite. Finally, nanostructured Cr-based WC hardmetals have achieved superior performance than commercial Co-based WC hardmetals even with extra addition of refractory carbides, in terms of wear resistance. Furthermore, this Cr-based WC hardmetal will have a lower price and less toxicity than Co-based WC hardmetals. Therefore, Cr-based WC hardmetals seem to possess a bright future in the cutting tool industry, in applications in which high wear resistance is required.

Acknowledgements

References

[1] S. Norgren, J. García, A. Blomqvist, L. Yin, Trends in the P/M hard metal industry, Int. J. Refract. Met. Hard Mater. 48 (2015) 31–45.
[2] M. Tkadletz, N. Schalk, R. Daniel, J. Keckes, C. Czettl, C. Mitterer, Advanced characterization methods for wear resistant hard coatings: a review on recent progress, Surf. Coatings Technol. 285 (2016) 31–46.
[3] K. Jia, T.E. Fischer, Abrasion resistance of nanostructured and conventional cemented carbides, Wear. 200 (1996) 206–214.
[4] Y. Liu, J. Cheng, B. Yin, S. Zhu, Z. Qiao, J. Yang, Tribology international study of the tribological behaviors and wear mechanisms of WC-Co and WC-Fe3Al hard materials under dry sliding condition, Tribiology Int. 109 (2017) 19–25.
[5] K. Bonny, P. De Baets, J. Vleugels, S. Huang, O. Van Der Biest, B. Lauwers, Impact of Cr3C2/VC addition on the dry sliding friction and wear response of WC-Co cemented carbides, Wear. 267 (9–10) (2009) 1642–1652.
[6] K. Bonny, P. De Baets, Y. Perez, J. Vleugels, B. Lauwers, Friction and wear characteristics of WC-Co cemented carbides in dry reciprocating sliding contact, Wear. 268 (11–12) (2010) 1504–1517.
[7] R.B. Bhagat, J.C. Conway, M.F. Amateau, R.A. Brezler, Tribological performance evaluation of tungsten carbide-based cermets and development of a fracture mechanics wear model, Wear. 102 (12) (1996) 233–243.
[8] C. Allen, M. Sheen, J. Williams, V.A. Pugsley, The wear of ultrafine WC-Co hard metals, Wear. 250 (2001) 604–610.
[9] H. Saito, A. Iwabuchi, T. Shimizu, Effects of Co content and WC grain size on wear of WC cemented carbide, Wear. 261 (2006) 126–132.
[10] V.B. Voitovich, V.V. Sverdel, R.F. Voitovich, E.I. Golovko, I.N. Frantsevich, Oxidation of WC-Co, WC-Ni and WC-Co-Ni hard metals in the temperature range 500 ~ 800 °C, Int. J. Refract. Met. Hard Mater. 14 (4) (1996) 289–295.
[11] M. Aristizabal, J.M. Sanchez, N. Rodriguez, F. Ibarreta, R. Martinez, Comparison of the oxidation behaviour of WC-Co and WC-Ni-Co-Cr cemented carbides, Corros. Sci. 53 (9) (2011) 2754–2760.
[12] A. Bautista, F. Velasco, J. Abenojar, Oxidation resistance of sintered stainless steels : effect of yttria additions, Corros. Sci. 45 (6) (2003) 1343–1354.
[13] J. Larsen-Basse, Effect of composition, microstructure, and service conditions on the wear of cemented carbides, JOM. 35 (11) (1983) 35–42.
[14] D.G.F. Oquigley, S. Luyckx, M.N. James, An empirical ranking of a wide range of WC-Co grades in terms of their abrasion resistance measured by the ASTM standard B 611-85 test, Int. J. Refract. Met. Hard Mater. 15 (1–3) (1997) 73–79.
[15] S.I. Cha, S.H. Hong, G.H. Ha, B.K. Kim, Microstructure and mechanical properties of nanocrystalline WC-10Co cemented carbides, Scr. Mater. 44 (3) (2001) 1535–1539.
[16] K. Jia, T.E. Fischer, Sliding wear of conventional and nanostructured cemented carbides, Wear. 204 (1997) 310–318.
[17] S.G. Huang, L. Li, K. Vanmeensel, O. Van Der Biest, J. Vleugels, VC, Cr3C2 and NbC doped WC-Co cemented carbides prepared by pulsed electric current sintering, Int. J. Refract. Met. Hard Mater. 25 (5–6) (2007) 417–422.
[18] L.H. Zhu, Q.W. Huang, H.F. Zhao, Preparation of nanocrystalline WC-10Co-0.8 VC by spark plasma sintering, J. Mater. Sci. Lett. 22 (22) (2003) 1631–1633.
[19] D. Sivaprahasam, S.B. Chandrasekar, R. Sundaresan, Microstructure and mechanical properties of nanocrystalline WC-12Co consolidated by spark plasma sintering, Int. J. Refract. Met. Hard Mater. 25 (2) (2007) 144–152.
[20] V. Bounhoure, S. Lay, S. Coindeau, S. Norgren, E. Pauty, J.M. Missiaen, Effect of Cr addition on solid state sintering of WC-Co alloys, J. Refract. Hard Mater. 52 (2015) 21–28.
[21] X.X. Deng, J.M. Torralba, A. García-Junceda, Field-Assisted Sintering of WC Hardmetals with Cr-Based Binder, Euro PM2017 Congress & Exhibition, Milan, Italy, 2017 (978-1-899072-49-1).
[22] A. García-Junceda, I. Sáez, X.X. Deng, J.M. Torralba, Development of a Cr-based hard composite processed by spark plasma sintering, Metall. Mater. Trans. A 49 (4) (2018) 1363–1371.
[23] H. Engqvist, B. Uhrenius, Determination of the average grain size of cemented carbides, Int. J. Refract. Met. Hard Mater. 21 (1–2) (2003) 31–35.
[24] X.X. Deng, D. Garbiec, J.Y. Wang, J.M. Torralba, A. García-Junceda, Development of Cr-Based Hardmetals by Spark Plasma Sintering: Thermodynamic Modeling and Hardness/Toughness Assessment, Euro PM2018 Congress & Exhibition, Bilbao, Spain, 2018 (978-1-899072-50-7).
[25] Z. Doni, A.C. Alves, F. Toptan, J.R. Gomes, A. Ramalho, M. Buciumeanu, Dry sliding and tribocorrosion behaviour of hot pressed CoCrMo biomedical alloy as compared with the cast CoCrMo and Ti6Al4V alloys, Mater. Des. 52 (2013) 47–57.
[26] J.K. Lancaster, The influence of substrate hardness on the formation and endurance of molybdenum disulphide films, Wear. 10 (2) (1966) 103–117.
[27] A.T. Fry, P. Lovelock, N. Smith, M. Gee, A.J. Gant, An innovative high temperature solid particulate erosion testing system, Wear. 376-377 (2017) 458–467.
[28] L.M. Vilhena, C.M. Fernandes, E. Soares, J. Sacramento, A.M.R. Senos, A. Ramalho, Abrasive wear resistance of WC-Co and WC-AISI 304 composites by ball-cratering method, Wear. 346 (2016) 99–107.
[29] C. Pignie, M.G. Gee, J.W. Nunn, H. Jones, A.J. Gant, Simulation of abrasion to WC/Co hardmetals using a micro-tribology test system, Wear. 302 (1–2) (2013) 1050–1057.
[30] B. Yaman, H. Mandal, Wear performance of spark plasma sintered Co/WC and cBN/co/WC composites, Int. J. Refract. Met. Hard Mater. 42 (2014) 9–16.
[31] L. Espinosa, V. Bonache, M.D. Salvador, Friction and wear behaviour of WC-Co-Cr3C2-VC cemented carbides obtained from nanocrystalline mixtures, Wear. 272 (1) (2011) 62–68.